

# Fluorescence Quenching of Single-Walled Carbon Nanotubes in SDBS Surfactant Suspension by Metal Ions: Quenching Efficiency as a Function of Metal and Nanotube Identity<sup>†</sup>

Jonathan J. Brege, Clayton Gallaway, and Andrew R. Barron\*

Richard E. Smalley Institute for Nanoscale Science and Technology, Carbon Nanotube Laboratory, and Department of Chemistry, Rice University, Houston, Texas 77005

Received: February 14, 2007; In Final Form: July 7, 2007

The effects of both the metal ion and the counterion on the fluorescence of SDBS-surfacted single-walled carbon nanotubes (SWNTs) have been investigated for solutions of group 2, 12, and 13 metal salts with a  $[M^{n+}]$  of between 0.5 and 5 mM per 15 mg.L<sup>-1</sup> of SWNT. The following metal salts cause a decrease in fluorescence of the SWNTs: MgCl<sub>2</sub>, Mg(SO<sub>4</sub>), Mg(OAc)<sub>2</sub>, CaCl<sub>2</sub>, Ca(OAc)<sub>2</sub>, SrCl<sub>2</sub>, BaCl<sub>2</sub>, Ba(OAc)<sub>2</sub>, Zn(SO<sub>4</sub>), CdCl<sub>2</sub>, Cd(SO<sub>4</sub>), Cd(OAc)<sub>2</sub>, HgCl<sub>2</sub>, and Hg(OAc)<sub>2</sub>. In contrast, Ga<sub>2</sub>(SO<sub>4</sub>)<sub>3</sub>, and Al(NO<sub>3</sub>)<sub>3</sub> show no reduction in fluorescence over the concentration range studied. The decrease in fluorescence is found to be due to quenching rather than bundling, acid suppression, or spectral bleaching. The Stern–Volmer quenching constants are found to depend on the identity of the metal ion, the anion, and the diameter (related to the  $n,m$  value) of the SWNT. For group 2 metals, the quenching efficiency follows the trend of increasing ionic radii (Mg < Ca < Sr < Ba), whereas the relationship between the group 12 metals is more complex (Zn < Cd ≥ Hg). Overall there is a dependence on the ionic radius of the metal: ions with a radius less than 1 Å exhibit little quenching, but those with radii greater than 1 Å show increasing quenching efficiency with increased size. With regard to the counterion, the quenching efficiency follows the trend of Cl<sup>-</sup> ≈ SO<sub>4</sub><sup>2-</sup> < OAc<sup>-</sup>. The Stern–Volmer quenching constants for a particular metal/anion combination show a linear correlation with the SWNT band gap and an inverse, but equal, relationship for the diameter of the SWNT. The formation of a nonfluorescent ground-state complex or spectral bleaching may be precluded as possible mechanisms for the quenching, but there is clearly a perturbation of the electronic structure of the SWNTs as indicated by a change in the intensity of the radial breathing mode. We propose that the SWNT exciton formed from light absorption is sensitive to its local environment and that the field around the metal ions has a significant effect on the exciton facilitating nonradiative decay paths. The lack of quenching caused by Al<sup>3+</sup> and Ga<sup>3+</sup> salts is consistent with either their speciation as M(OH)<sub>4</sub><sup>-</sup> ions under the conditions employed or the effect on the SWNT exciton being related to charge density.

## Introduction

Single-walled carbon nanotubes (SWNTs) can be either metallic or semiconducting, depending on their helicity and diameter.<sup>1</sup> The fundamental optical and electronic properties of SWNTs are closely related to their chiral wrapping angle: designated by the  $n,m$  indices. Cases where  $(n-m)$  are not divisible by 3 are semiconducting with bandgaps dependent on the helicity (and hence diameter) of the tube. The optical properties of individual semiconducting SWNTs have been studied extensively, and specific chirality tubes have been assigned specific emission wavelengths.<sup>1</sup> Unlike most single molecules<sup>2</sup> or other nanomaterials such as quantum dots,<sup>3</sup> SWNTs exhibit no fluctuations in fluorescence intensity or spectral changes, making them attractive fluorophores for sensing applications. The properties of the various  $n,m$  tubes are sensitive to their surrounding environment. Charge-transfer processes have been investigated through fluorescence-quenching experiments. It has been shown that O<sub>2</sub>, NO<sub>2</sub>, and NH<sub>3</sub> can accept or donate electrons to the tubes, causing changes in the

electronic structure.<sup>4,5</sup> Such properties make SWNTs ideal for nanoscale sensing applications.<sup>6</sup>

It has been reported that the bleaching of nanotube fluorescence and absorbance spectra from the reaction of surfacted SWNTs with small organic electron-acceptor molecules depends solely on the reduction potential of the organic molecule.<sup>7</sup> The quenching ability of a particular organic species for a specific chirality tube is controlled by the reduction potential of the dye and the band gap of the tube. The bleaching is selective because tubes with bandgaps above a threshold energy are affected, whereas those under the threshold are unaffected. In these results, SWNTs can be perceived as behaving in a manner similar to that of other fluorescent organic molecules. Metal ions have been used in emission studies to quench the fluorescence of various organic molecules including pyrenes, anthracenes, flavins, bipyridines, and acridinium ions.<sup>8,9,10,11</sup> Thus far, no work has concentrated on the interactions between SWNTs and metal ions, although Doorn and co-workers have recently reported that the addition of NaCl or MgCl<sub>2</sub> to sodium dodecylsulfate (SDS) surfacted SWNTs promotes the selective aggregation of the SWNTs.<sup>12</sup> As part of our prior studies in coating SWNTs with CdS,<sup>13</sup> we observed that the fluorescence of surfacted SWNTs was quenched with the addition of Cd<sup>2+</sup>/

<sup>†</sup> Part of the special issue "Richard E. Smalley Memorial Issue".

\* Corresponding author. Address: Department of Chemistry, Rice University, MS-60, 6100 Main Street, Houston, TX 77005. E-mail: arb@rice.edu.

NH<sub>4</sub>OH/TEA prior to the addition of the sulfur source (thiourea). Upon addition of thiourea, and the formation of CdS coatings, the fluorescence returned to its original intensity. Thus, it would appear that Cd<sup>2+</sup> quenches the SWNT fluorescence. In order to further explore this phenomenon and determine the generality of M<sup>n+</sup> quenching of SWNT fluorescence, we have investigated the charge-transfer reaction between sodium dodecylbenzenesulfonate (SDBS) surfactant SWNTs with group 2, 12, and 13 metal ions. Stern–Volmer constants were obtained for each of the metals with 18 different chirality nanotubes.

### Experimental Section

All chemicals were obtained commercially and used without further purification. All solutions used contained ultrapure (UP) water from a Millipore Milli-Q UV water filtration system. HiPco SWNTs (batch 162.10) were obtained from the Carbon Nanotube Laboratory (Rice University, Houston, TX). Metal salts used were Al(NO<sub>3</sub>)<sub>3</sub> (Mallinckrodt Chemical), Ga<sub>2</sub>(SO<sub>4</sub>)<sub>3</sub> (Strem Chemicals), HgCl<sub>2</sub> (EM Science), BaCl<sub>2</sub> (Merck), Hg(OAc)<sub>2</sub> and MgCl<sub>2</sub> (J.T. Baker Chemical Company), CdCl<sub>2</sub>, Cd(SO<sub>4</sub>), Cd(OAc)<sub>2</sub>, Ca(OAc)<sub>2</sub>, and Zn(SO<sub>4</sub>)<sub>7</sub>(H<sub>2</sub>O) (Sigma-Aldrich), and Ba(OAc)<sub>2</sub>, CaCl<sub>2</sub>, Mg(SO<sub>4</sub>), Mg(OAc)<sub>2</sub>, and SrCl<sub>2</sub> (Fisher Scientific Company). Technical-grade sodium dodecylbenzenesulfonate (SDBS), 99.5% EDTA (Sigma-Aldrich), and 14.8 N NH<sub>4</sub>OH (Fisher Scientific Company) were used as received. Fluorescence spectra were collected on a NanoSpectralyzer (Applied NanoFluorescence, LLC) with 660- and 785-nm excitation sources, Raman data was obtained using a Kaiser Process Raman spectrometer (Kaiser Optical Inc.) with 785-nm excitation. Absorption spectra were collected on a Varian Cary 400 spectrophotometer. All measurements were taken at room temperature (298 K).

**Preparation of Surfactant Nanotubes.** Solutions of SDBS surfactant SWNTs (SDBS-SWNTs) were prepared using a modification of procedures published previously.<sup>14</sup> Raw HiPco SWNTs were dispersed in SDBS solution (225 mL, 1%) and sonicated for 15 min in a cup-horn sonicator (Cole Palmer CPX-600, 540 W). The solution was centrifuged (Sovall 100S Discovery Ultracentrifuge with Surespin 630 swing bucket rotor) for 4 h at 122 000 G. The top 2/3 of the solution was decanted off (referred to as surf-tubes) and diluted with 1% surfactant solution to obtain a concentration of 24 mg·L<sup>-1</sup> as determined by UV–vis spectroscopy.

**Fluorescence Quenching of Surfactant Nanotubes.** NH<sub>4</sub>OH (4 M, 0.4 mL per 1.0 mL of surf-tubes) was added to the surf-tubes and stirred for 24 h. The NH<sub>4</sub>OH/SDBS-SWNTs were placed in a cuvette (2.8 mL), and 0.4 mL of metal solution (concentration varying from 0 to 40 mM in 4 mM increments) was added. The solution was inverted several times to induce mixing. The final concentrations were 15 mg·L<sup>-1</sup> surfactant nanotubes, 1 M NH<sub>4</sub>OH, and 0–5 mM (in 0.5 mM increments) metal ions. After 1 h, fluorescence measurements were obtained by 660- and 785-nm excitation and absorption spectra were collected. The pH of each NH<sub>4</sub>OH/SDBS-SWNT/M<sup>n+</sup> combination was obtained using pH-indicator strips to ensure that the pH had not changed by more than 0.5 pH units. Fluorescence spectra were automatically fitted with ANF NanoSpectralyzer software to yield excitation profiles of 43 different nanotubes. The 18 most-intense peaks were chosen for analysis. Stern–Volmer plots were prepared by graphing ( $I_0/I$ )-1 versus [M<sup>n+</sup>] where  $I_0$  is the intensity of the NH<sub>4</sub>OH-tubes in absence of the metal ion,  $I$  is the intensity of the NH<sub>4</sub>OH-tubes with the metal ion present, and [M<sup>n+</sup>] is the concentration of the metal solution in moles per liter. A linear least-squares regression was performed to obtain the Stern–Volmer constants.

Sodium hydroxide (pH = 12.5, 0.4 mL per 1.0 mL of SDBS-SWNTs) was added to the SDBS-SWNT solution and stirred for 24 h. The NaOH/SDBS-SWNT solution (2.8 mL) was placed in a cuvette, and the appropriate metal solution (0.4 mL, concentration varying from 0 to 40 mM in 4 mM increments) was added. The solution was inverted several times to induce mixing. The final concentrations were 15 mg·L<sup>-1</sup> surfactant nanotubes, and 0–5 mM in 0.5 mM increments of metal ions. After 1 h, fluorescence measurements were obtained by 660- and 785-nm excitation and absorption spectra were collected. The pH of each NaOH/SDBS-SWNT/M<sup>n+</sup> combination was obtained using pH-indicator strips. It was found that the metal ions reacted with the strong base, changing the pH. In addition to the metal ions, the change in pH also causes quenching (see below); therefore, NaOH was found to not be a suitable base for these quenching studies.

**Nanotube Fluorescence as a Function of pH.** To ensure that the pH did not play a role in the quenching mechanism, we placed SDBS-SWNTs (2.0 mL, 24 mg·L<sup>-1</sup>) in a cuvette. NH<sub>4</sub>OH solution (0.8 mL, pH = 7.5) was added, and the solution was inverted several times to mix. Fluorescence measurements were taken after 24 h. The process was repeated for NH<sub>4</sub>OH solutions with pH = 7.5–12.5 in 0.5 pH unit increments, and the fluorescence intensity was monitored.

**Fluorescence Recovery.** For fluorescence recovery experiments, three solutions were prepared. A blank was prepared by placing NH<sub>4</sub>OH/SDBS-SWNTs (2.1 mL, 1:0.4 ratio) in a cuvette. Millipore water (0.3 mL) was added, and the cuvette was inverted several times to induce mixing. After 30 min, EDTA solution (0.3 mL, 100 mM in 1 M NH<sub>4</sub>OH) was added, and the solution was mixed. Fluorescence measurements were obtained 30 min later. Samples of metal-ion-quenched SWNTs were obtained by combining NH<sub>4</sub>OH/SDBS-SWNT (2.1 mL, 1:0.4 ratio) with metal solution (0.3 mL) in a cuvette, where the concentration of the solution is dependent on the type of metal. The concentration was chosen to quench the fluorescence of the SWNTs to approximately 2/3 of their original intensity. The cuvette was inverted several times and set for 30 min. NH<sub>4</sub>OH solution (0.3 mL, 1 M) was added, and the solution was mixed. Fluorescence measurements were obtained after 30 min. Fluorescence recovered samples were made by combining NH<sub>4</sub>OH/SDBS-SWNT (2.1 mL, 1:0.4 ratio) with metal solution (0.3 mL) in a cuvette, where the concentration of the solution is dependent on the type of metal. The cuvette was inverted several times and set for 30 min. EDTA solution (0.3 mL, 100 mM in 1 M NH<sub>4</sub>OH) was added, the cuvette was inverted several times, and fluorescence measurements were obtained after another 30 min. Spectra were compared to the blank to the metal-ion-quenched SWNTs.

**Quenching Mechanism.** Fluorescence-quenching processes are described by the Stern–Volmer equation ( $I_0/I = K_{SV}[Q] + 1$ ), where  $K_{SV} = k_q\tau_0$ ,  $K_{SV}$  is the Stern–Volmer (SV) quenching constant,  $k_q$  is the quenching rate constant (M<sup>-1</sup>sec<sup>-1</sup>), and  $\tau_0$  is the excited singlet lifetime of the fluorophore in the absence of a quencher.

**Raman Monitoring.** The fluorescence of NH<sub>4</sub>OH/SDBS-SWNTs with the metal-ion solutions was monitored over time using Raman spectroscopy. NH<sub>4</sub>OH/SDBS-SWNTs (2.1 mL, 1:0.4 ratio) were placed in a cuvette. While stirring, in situ Raman measurements were taken every 45 s (1 s exposure, 5 accumulations). After 5 min, the appropriate metal solution (0.3 mL, 20 mM) was added to the cuvette and spectra were collected for 6 h. Changes in electron density in the SWNTs were monitored using Raman spectroscopy. NH<sub>4</sub>OH/SDBS-

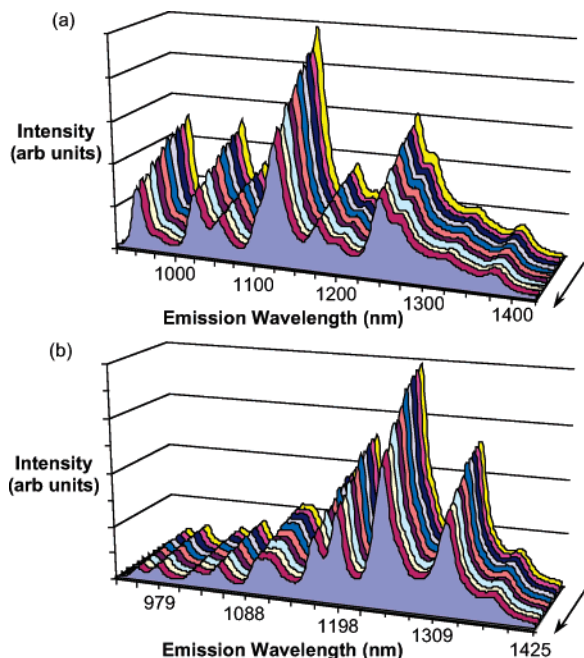


**Figure 1.** Fluorescence spectra of SDBS-SWNTs in the presence of  $\text{Cd}(\text{OAc})_2$  with (a) 660-nm and (b) 785-nm excitation showing the decrease in fluorescence with increased  $\text{Cd}^{2+}$  concentration (0–5.0 mM in 0.5 mM steps). The arrows indicate increasing  $\text{Cd}^{2+}$  ion concentration.

SWNTs (2.1 mL, 1:0.4 ratio) were placed in a cuvette. While stirring, in situ Raman measurements were taken every 45 s (with 1 s exposure, 5 accumulations). After 5 min, the metal solution (0.3 mL, 20 mM) was added to the cuvette and spectra were collected for 30 min. EDTA solution (0.3 mL, 100 mM in 1 M  $\text{NH}_4\text{OH}$ ) was added, and spectra were taken for 5 additional minutes.

## Results and Discussion

Individual semiconducting SWNTs dispersed in SDBS surfactant exhibit fluorescence from 660- and 785-nm irradiation.<sup>15</sup> In agreement with our prior studies,<sup>13</sup> the addition of cadmium acetate solution with a  $[\text{Cd}^{2+}]$  value between 0.5 and 5.0 mM per 15  $\text{mg}\cdot\text{L}^{-1}$  of SWNTs results in the reduction of the fluorescence of the SWNTs. As shown in Figure 1, each of the different fluorescing  $n,m$  nanotubes is affected by the presence of the  $\text{Cd}^{2+}$  ions, and all of the semiconducting nanotubes exhibit a decrease in fluorescence intensity with increasing metal-ion concentration. The three-dimensional plots indicate that the decay is monotonic and appears to be independent of the excitation energy (see below). Weisman and co-workers have shown that the fluorescence spectra may be fitted for the contributions from each particular  $n,m$  SWNT.<sup>16</sup> Each individual spectrum was therefore fitted to determine the intensity contributions of 43 different fluorescing tubes (see the Experimental Section). Analysis of a spectrum in the presence and absence of  $\text{Cd}^{2+}$  shows that there is no shift in the emission wavelengths, see Figure 2.

Given the well-behaved decrease in fluorescence of the SWNTs by  $\text{Cd}^{2+}$  using  $\text{Cd}(\text{OAc})_2$ , we have investigated the effects of both the metal ion and the counterion for metal-salt solutions with a  $[\text{M}^{n+}]$  value of between 0.5 and 5 mM per 15  $\text{mg}\cdot\text{L}^{-1}$  of SWNT. The following metal salts cause an analogous decrease in fluorescence of the SWNTs (albeit with varying efficiencies per millimole of  $\text{M}^{n+}$ ):  $\text{MgCl}_2$ ,  $\text{Mg}(\text{SO}_4)$ ,  $\text{Mg}(\text{OAc})_2$ ,  $\text{CaCl}_2$ ,  $\text{Ca}(\text{OAc})_2$ ,  $\text{SrCl}_2$ ,  $\text{BaCl}_2$ ,  $\text{Ba}(\text{OAc})_2$ ,  $\text{Zn}(\text{SO}_4)$ ,

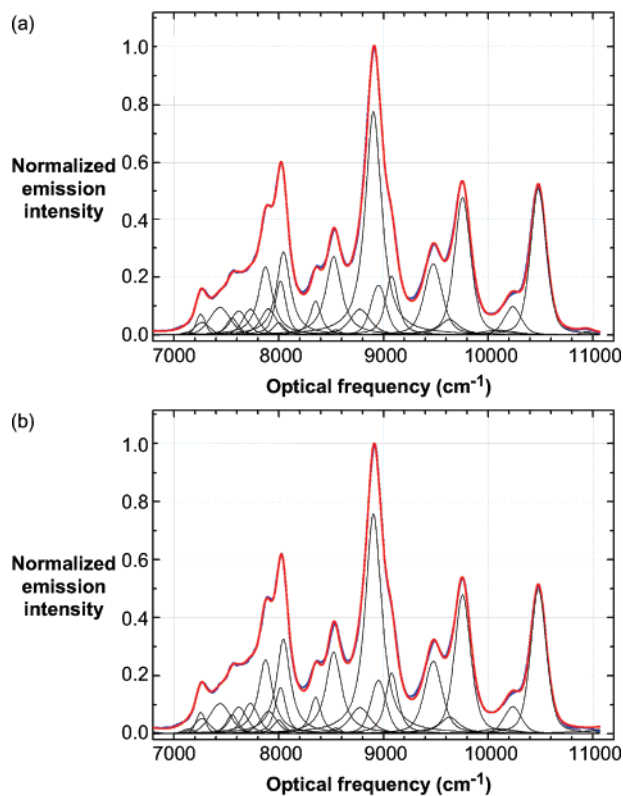


**Figure 2.** Deconvoluted fluorescence spectra (660-nm excitation) of (a) SDBS-SWNTs and (b) SDBS-SWNTs in the presence of  $\text{Cd}(\text{OAc})_2$  (4.0 mM), showing the measured (blue line) and simulated (red line) spectra and the basis functions (black line). The spectra are normalized to allow comparison of the spectral deconvolutions.

$\text{CdCl}_2$ ,  $\text{Cd}(\text{SO}_4)$ ,  $\text{Cd}(\text{OAc})_2$ ,  $\text{HgCl}_2$ , and  $\text{Hg}(\text{OAc})_2$ . In contrast,  $\text{Ga}_2(\text{SO}_4)_3$ , and  $\text{Al}(\text{NO}_3)_3$  show no reduction in fluorescence over the concentration range studied.<sup>17</sup>

A decrease in fluorescence of a SWNT can be caused by any of several possible effects: intertube energy transfer from bundling, acid suppression of fluorescence, changes in the absorption (spectral bleaching), and quenching via either static or dynamic mechanisms. Prior to further studies of metal, counterion, and SWNT  $n,m$  effects, it is worth discussing the possibility each of these alternatives.

Individual semiconducting SWNTs suspended in solution fluoresce when a sufficient micellar layer is present to provide isolation from other SWNTs (in particular, the metallic ones).<sup>14</sup> Disruption of the micelle structure allows for van der Waals attractions to dominate, resulting in bundling of the SWNTs and thus a decrease in fluorescence intensity. Subsequent bundling is irreversible without extreme physical treatment such as sonication.<sup>18</sup> On the basis of these observations, we propose that in the present case bundling does not occur. First, at extreme ionic strengths, the surfactant micelle structure can be perturbed. However, addition of  $\text{Na}^+$ ,  $\text{Cs}^+$ ,  $\text{Al}^{3+}$ , or  $\text{Ga}^{3+}$  does not change the fluorescence even though they were used in the same concentration as the other metals that do affect fluorescence (i.e.,  $\text{Cd}^{2+}$ ). Second, a characteristic of bundling of SWNTs is a red shift and broadening of the bands in the UV–vis spectrum.<sup>14</sup> As can be seen from Figure 3, no such effects occur with the addition of  $\text{Cd}^{2+}$ , suggesting that the ground-state electronic structure of the SWNTs is not perturbed. Finally, in our original report with the formation of  $\text{CdS}$ -coated SWNTs, we observed that the fluorescent intensity was regained upon addition of the sulfur source (thiourea), which we proposed was

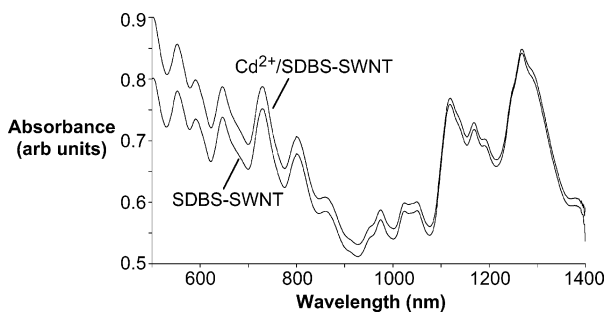


**Figure 3.** UV-vis absorption spectra of (a) SDBS-SWNTs and (b) SDBS-SWNTs in the presence of  $\text{CdCl}_2$  (2.0 mM).

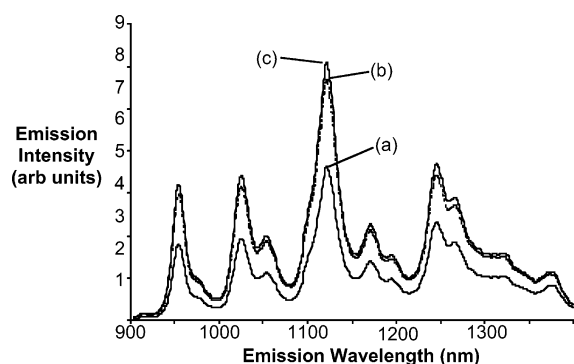


**Figure 4.** Fluorescence of SDBS-SWNTs using 660-nm excitation in the presence of  $\text{SrCl}_2$  (3.0 mM) before (a) and after (b) the addition of EDTA (15 mM) showing the recovery of fluorescence with the addition of EDTA. The fluorescence spectrum with EDTA (15 mM) in the absence of quencher molecules is shown for comparison (c).

due to the removal of the  $\text{Cd}^{2+}$  ion from the surface of the SWNT. As an alternative to reacting the metal ion, complexation with a chelate agent should have the same effect. Indeed, fluorescence loss due to the presence of  $\text{M}^{n+}$  ions can be recovered by adding EDTA. For example, as may be seen from Figure 4, addition of 3.0 mM  $\text{SrCl}_2$  to SDBS-SWNTs results in a reduction in fluorescence. Subsequent addition of an excess of EDTA results in the recovery of fluorescence (Figure 4). It is important to note that if the SWNTs did bundle the binding energy of  $\sim 0.5 \text{ eV}\cdot\text{nm}^{-1}$  of SWNT contact is difficult to overcome and treatment with EDTA would not separate them. On the basis of the foregoing, it is clear that the observed fluorescence loss is not due to nanotube bundling.

Smalley and co-workers have shown that SWNT fluorescence is suppressed in an acidic medium.<sup>19</sup> In addition, dissolved oxygen can cause a reduction in SWNT fluorescence, but only when  $\text{H}^+$  is present.<sup>5,20</sup> Both of these issues are overcome by the use of basic conditions. In this study, we adjusted the solution with  $\text{NH}_4\text{OH}$  for several reasons. First, the basic medium eliminates large quantities of hydronium ion being present in solution prohibiting fluorescence loss from dissolved oxygen, allowing the reactions to be run in air. Second, the use of  $\text{NaOH}$  as a source of base resulted in a significant change in pH with the addition of the metal ions. For example, addition of 5.0 mM  $\text{CdCl}_2$  to a  $\text{NaOH/SDBS-SWNT}$  solution results in a reduction of pH from 10.5 to 7.5. Such a change in pH results in significant decreases in the fluorescence of the SWNTs. We are interested in the fluorescence decrease caused by the presence of the  $\text{M}^{n+}$  ions; therefore, using  $\text{NH}_4\text{OH}$  resulted in the pH remaining constant (pH = 10.5) with the addition of  $\text{M}^{n+}$ , indicating that fluorescence loss is not due to a pH change.

A loss of SDBS-SWNT fluorescence can be caused by changes in the absorption properties of the fluorophores. Previous reports indicate that there is an absorbance reduction

(in concert with fluorescence decay) when organic molecules react with SWNTs.<sup>7</sup> This process is ordinarily classified as “spectral bleaching”. As may be seen from Figure 3, there is no change in the absorbance spectra accompanying fluorescence decay with the addition of metal ions ( $\text{Cd}^{2+}$  in Figure 3), indicating that spectral bleaching is not the source of fluorescence decay.

On the basis of the above evidence, we propose that the decrease in fluorescence of the SDBS-SWNTs in the presence of  $\text{M}^{n+}$  is not caused by bundling, acid suppression, or spectral bleaching, and must therefore be due to quenching. The fluorescence quenching of SDBS-SWNTs by  $\text{M}^{n+}$  is consistent with Stern–Volmer behavior, and therefore we can characterize the quenching of individual nanotubes. Fluorescing species with intensity  $I_0$ , quenched by a species  $\text{M}^{n+}$ , to give a reduced intensity  $I$ , follow eq 1, where  $K_{\text{SV}}$  is the Stern–Volmer quenching constant.

$$I_0/I = K_{\text{SV}}[\text{M}^{n+}] + 1 \quad (1)$$

In this manner, we can obtain the Stern–Volmer quenching constants using a linear regression least-squares fit for each metal, counterion, and SWNT  $n,m$  combination (Tables 1 and 2). Figure 5 shows a representative Stern–Volmer plot for quenching of a 6,5-SWNT by  $\text{Hg}(\text{OAc})_2$ . Some of the  $n,m$  SWNTs are either absent from the sample, not strong emitters with the excitation energies used, or are in a low percentage and have a minimal intensity contribution to the overall spectrum. Consequently, preparing meaningful Stern–Volmer plots from these  $n,m$  SWNTs is not possible. For these reasons, we analyzed the 18 most-intense nanotubes present in the sample.

It has been reported previously that there is an excitation-wavelength dependence on the fluorescence quenching of functionalized SWNTs by nitroaromatic molecules.<sup>21</sup> We observe minimal excitation dependence with only slight variations in the quenching processes from 660- and 785-nm excitation (see Tables 1 and 2). This is expected, however, because the dependence is most-prominent at low excitation wavelengths and diminishes at high wavelengths.

**Dependence on Metal.** As may be seen from Tables 1 and 2, the quenching constant for a particular  $n,m$  SWNT is highly dependent on the choice of metal ion and counterion. A comparison of the data for the chloride salts (thus eliminating counterion effects) for the quenching of the 10,2 SDBS-SWNT (Figure 6) shows that within the group 2 metals the quenching efficiency follows the trend of increasing atomic number (i.e.,  $\text{Mg} < \text{Ca} < \text{Sr} < \text{Ba}$ ). The relationship between the group 12 metals is a little more complex. Although the Stern–Volmer quenching constants for  $\text{Zn}(\text{SO}_4)$  are all significantly less than the analogous values for  $\text{Cd}(\text{SO}_4)$ , the values for  $\text{Hg}(\text{OAc})_2$  are within experimental error of those of  $\text{Cd}(\text{OAc})_2$  (Figure 7a) rather than larger as would be expected by the trend observed for the group 2 metals. Furthermore, the quenching constants for  $\text{HgCl}_2$  are significantly lower than those for  $\text{CdCl}_2$  (Figure 7b). Comparing the data for all of the  $n,m$  values, it is apparent that there is no correlation between the Stern–Volmer quenching constant and the atomic number, diffusion coefficient, UV-vis spectral overlap, or the reduction potential. As may be seen from Figure 8, there is, however, an apparent dependence of on the ionic radius of the quenching metal. Importantly, ions with a radius less than 1 Å exhibit little quenching, but those with radii greater than 1 Å show increasing quenching efficiency with increased size. The slight anomaly of this trend is the mercury derivatives that appear to be consistent with an apparent

**TABLE 1: Calculated Quenching Constants for Group 2 Metal Complexes from 660- and 785-nm Irradiation<sup>a</sup>**

complex	SWNT <i>n,m</i>																	
	10,6	12,4	9,7	13,2	14,0	8,7	10,5	9,5	8,6	12,1	9,2	7,6	8,4	9,4	10,2	7,5	6,5	8,3
MgCl <sub>2</sub>	30 (29)	21 (20)	27 (26)	11 (11)	19 (19)	30 (30)	27 (26)	6.1 (5.2)	24 (23)	33 (32)	21 (21)	31 (30)	35 (34)	26 (26)	28 (28)	31 (30)	36 (35)	30 (29)
MgSO <sub>4</sub>	16 (11)	22 (17)	18 (12)	22 (16)	18 (13)	21 (16)	21 (15)	14 (8.0)	30 (24)	18 (12)	15 (9.3)	43 (36)	20 (14)	26 (20)	33 (27)	39 (32)	36 (30)	36 (30)
Mg(OAc) <sub>2</sub>	27 (21)	37 (32)	31 (26)	34 (29)	33 (28)	27 (21)	33 (27)	32 (27)	43 (37)	29 (23)	23 (18)	55 (48)	34 (29)	42 (36)	47 (41)	50 (44)	51 (45)	54 (48)
CaCl <sub>2</sub>	8.7 (3.9)	25 (19)	40 (34)	40 (34)	13 (7.9)	32 (26)	41 (35)	26 (21)	43 (37)	28 (23)	38 (33)	61 (54)	26 (21)	39 (33)	43 (37)	51 (45)	48 (42)	51 (45)
Ca(OAc) <sub>2</sub>	59 (56)	31 (30)	67 (64)	30 (28)	19 (18)	55 (53)	61 (58)	19 (17)	43 (42)	65 (62)	30 (28)	51 (49)	53 (51)	39 (37)	39 (38)	46 (45)	46 (45)	43 (43)
SrCl <sub>2</sub>	138 (128)	228 (215)	203 (190)	295 (281)	244 (231)	211 (199)	224 (211)	258 (245)	313 (298)	229 (216)	240 (227)	377 (361)	293 (278)	385 (368)	382 (366)	398 (381)	402 (385)	392 (375)
BaCl <sub>2</sub>	222 (204)	325 (304)	323 (301)	460 (433)	363 (340)	294 (274)	361 (338)	431 (406)	481 (454)	382 (358)	305 (285)	611 (579)	464 (437)	603 (572)	596 (565)	637 (604)	613 (581)	640 (607)
Ba(OAc) <sub>2</sub>	224 (206)	386 (363)	352 (330)	577 (548)	413 (389)	344 (322)	385 (362)	509 (482)	568 (539)	383 (360)	364 (341)	661 (630)	483 (457)	683 (650)	669 (637)	710 (677)	688 (655)	688 (655)

<sup>a</sup> Values for 785 nm given in parentheses.**TABLE 2: Calculated Quenching Constants for Group 12 Metal Complexes from 660- and 785-nm Irradiation<sup>a</sup>**

complex	SWNT <i>n,m</i>																	
	10,6	12,4	9,7	13,2	14,0	8,7	10,5	9,5	8,6	12,1	9,2	7,6	8,4	9,4	10,2	7,5	6,5	8,3
ZnSO <sub>4</sub>	19 (18)	17 (16)	<i>b</i>	<i>b</i>	6.5 (5.8)	<i>b</i>	<i>b</i>	3.3 (2.6)	13 (12)	<i>b</i>	24 (23)	19 (18)	4.8 (4.1)	7.1 (6.4)	12 (11)	13 (12)	21 (21)	12 (12)
CdCl <sub>2</sub>	31 (25)	42 (36)	47 (41)	45 (39)	30 (25)	49 (43)	50 (44)	38 (33)	58 (52)	51 (45)	70 (64)	72 (66)	56 (50)	63 (57)	64 (58)	69 (63)	79 (73)	73 (67)
Cd(SO <sub>4</sub> )	47 (41)	48 (43)	54 (49)	49 (44)	37 (31)	56 (51)	57 (52)	41 (35)	65 (59)	57 (52)	64 (58)	80 (73)	60 (54)	66 (60)	69 (63)	76 (70)	83 (76)	80 (74)
Cd(OAc) <sub>2</sub>	66 (60)	64 (58)	82 (75)	74 (68)	48 (42)	77 (70)	85 (78)	67 (61)	91 (84)	91 (84)	70 (64)	111 (103)	95 (88)	99 (91)	98 (90)	107 (99)	118 (110)	114 (106)
HgCl <sub>2</sub>	<i>b</i>	19 (16)	<i>b</i>	6.6 (3.9)	13 (10)	15 (12)	<i>b</i>	<i>b</i>	17 (14)	<i>b</i>	24 (21)	27 (23)	<i>b</i>	15 (12)	20 (17)	23 (20)	24 (21)	17 (14)
Hg(OAc) <sub>2</sub>	53 (45)	76 (67)	55 (47)	69 (61)	66 (58)	72 (64)	58 (50)	50 (42)	82 (73)	54 (46)	95 (86)	90 (81)	60 (52)	82 (73)	86 (77)	89 (80)	97 (88)	88 (79)

<sup>a</sup> Values for 785 nm given in parentheses. <sup>b</sup> Reliable quenching constants could not be obtained due to low intensity of peaks.

decrease in the effective radius of the Hg<sup>2+</sup> ion. Given the greater covalent nature of mercury compounds as compared to their Zn and Cd analogs, this may be a possible rationale for the reduced efficacy of the mercury compounds.

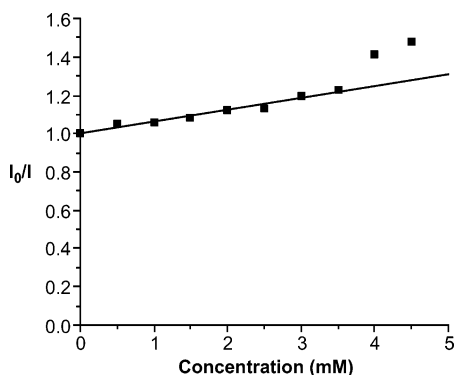
**Dependence on Anion.** In addition to the variation in the Stern–Volmer quenching constants with the identity of the metal ion, there is a lesser, but significant, dependence on the anion. As seen in Figure 9, the quenching efficiency follows the trend of Cl<sup>−</sup> ≈ SO<sub>4</sub><sup>2−</sup> < OAc<sup>−</sup>. Although it is unclear as to what the difference can be assigned to, we propose that although chloride and sulfate are noncoordinating anions (especially under the pH conditions employed herein), acetate would be expected to retain some coordination to the metal. The dependence on the identity of the counterion is distinct from quenching of organic fluorophores (e.g., 2,5-diphenylloxazole) by metal ions.<sup>8</sup>

**Dependence on SWNT *n,m*.** Figure 10 shows the Stern–Volmer quenching constants for SDBS-SWNTs as a function of SWNT *n,m* value in the presence of Ca(OAc)<sub>2</sub>. It is clear that there is a dependence of quenching on the identity of the SWNT (i.e., the *n,m* value).

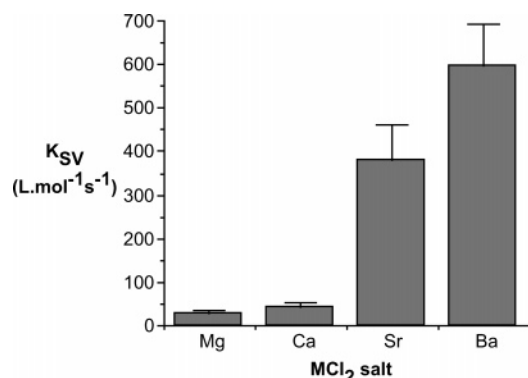
In previous studies, it has been reported that selective quenching between organic dyes and SWNTs of particular *n,m* values. This quenching occurs where the valance band of the SWNT is above a threshold value associated with the reduction potential of the dye.<sup>7</sup> Thus, for a particular SWNT/organic combination, SWNTs with a valance band above a certain value quench, whereas those with a valance band below that value do not. Such a situation does not occur for the quenching of SDBS-SWNTs by metal salts; however, as may be seen from

Figure 11a, a plot of the Stern–Volmer quenching constants for a particular metal/anion combination as a function of the SWNT band gap shows that within the error of the measurements a linear correlation exists. SWNTs with larger band gaps are quenched more efficiently than those with small band gaps. The variation between SWNTs of particular *n,m* values (i.e., the slope of the lines in Figure 11a) appears to depend on the relative ability of the metal as a quencher. Given that there is a near-inverse relationship between SWNT band gap and diameter, the inverse, but equal, relationships apply for the diameter of the SWNTs (Figure 11b).

**Possible Mechanisms of Quenching.** From the above discussion, we have found that the efficiency of a metal salt to quench the fluorescence of a SWNT depends on the ionic radius of metal, the identity of the counteranion, and the band gap and/or the diameter of the SWNT. Quenching reactions can be generally classified as either dynamic or static processes (or a combination of both).<sup>22</sup> Static quenching can be attributed to either the formation of a nonfluorescent ground-state complex or through a sphere of effective quenching. As noted above, the concentration dependence of the quenching follows a classic Stern–Volmer plot that is consistent with either static or dynamic mechanisms. We note that for some of the SWNT *n,m*/M<sup>n+</sup>/anion combinations there appears a positive deviation from linearity at high concentrations of the metal salt (see Figure 5). Such a deviation is suggestive of a more complex mechanism, making a definitive assignment of the mechanism difficult. However, we can preclude a simple static quenching mechanism involving the formation of a nonfluorescent ground state complex.



**Figure 5.** Representative Stern–Volmer plot for quenching of a 6,5-SDBS-SWNT by  $\text{Hg}(\text{OAc})_2$  measured using 660-nm excitation ( $R^2 = 0.969$ ).



**Figure 6.** Comparison of Stern–Volmer quenching constant for the 10,2-SDBS-SWNT with group 2 chlorides measured using 660-nm excitation.

If the SWNT and metal ion formed a nonfluorescent ground-state complex, then the electronic structure of the SWNT would be perturbed resulting in a red shift in the absorbance (e.g., Figure 3) and fluorescence spectra (e.g., Figures 1 and 2). As may be seen from Figures 1–3, no such red shift upon addition of  $\text{M}^{n+}$ . Thus, we propose that the quenching process does not involve the formation of a complex between the metal ion and the SWNT.

The reduced fluorescence reported for the dye-SWNT is attributed to spectral bleaching caused by electron transfer from the valance band of the SWNT to an acceptor molecule.<sup>7</sup> For such a ground-state process, electron transfer is expected to occur from the top of the SWNT valance band to the metal complex. Such an interaction would be particularly evident by changes in the characteristic first van Hove transitions.<sup>23</sup> As may be seen from Figure 3, the addition of a quenching  $\text{M}^{n+}$  does not result in any alteration of either the first (830–1600 nm) or second (600–800 nm) van Hove transitions,<sup>24</sup> indicating that the quenching process does not involve electron transfer from the valance band of the SWNT to an acceptor ion. Indeed, if it was a simple electron-transfer process then the quenching ability of the group 2 and 12 metal complexes would involve reduction of the metal centers or electron transfer into the lowest appropriate unfilled orbital on the metal•••solvate complex, most probably a  $\sigma^*$  orbital (i.e.,  $\text{M}-\text{NH}_3$  or  $\text{M}-\text{OH}_2$ ). The reduction potentials of each metal studied are significantly higher than the Fermi levels of the SWNTs.<sup>23</sup> Ab initio calculations of the relative energy of these orbitals indicate that these are also much higher than necessary to facilitate SWNT-to- $\text{M}^{n+}$  electron transfer.

In summary, the quenching process does not involve the formation of a complex between the metal ion and the SWNT

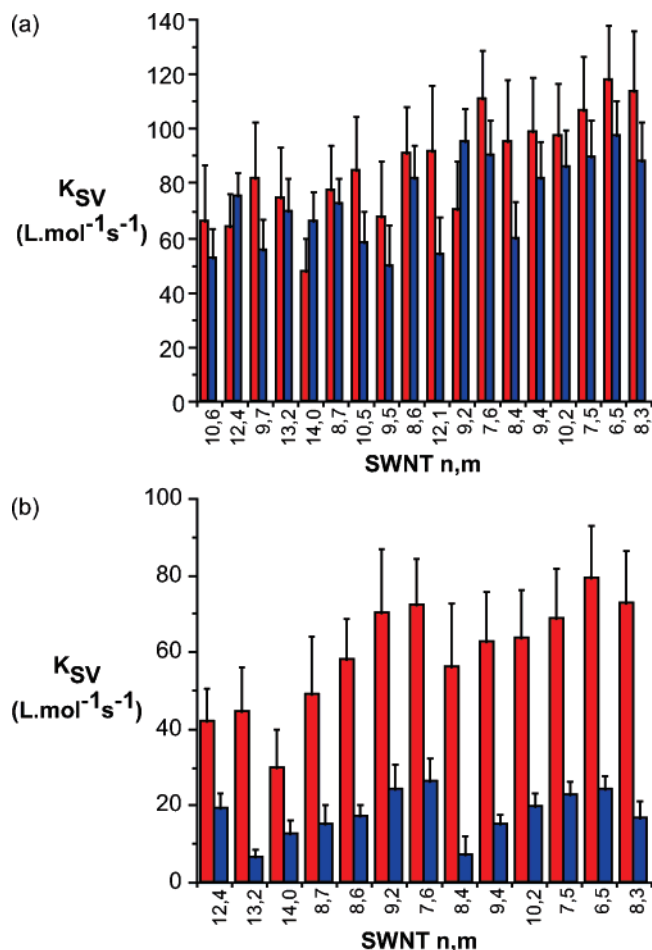


**Figure 7.** Comparison of Stern–Volmer quenching constant for selected SDBS-SWNTs  $n,m$  values (with increasing band gap from left to right) using 660-nm excitation with (a) chlorides of cadmium (red) and mercury (blue).

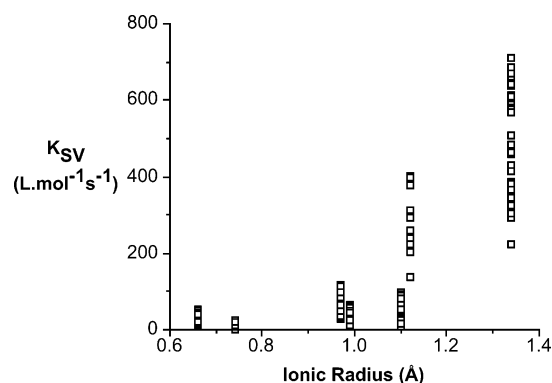


**Figure 8.** Stern–Volmer quenching constant for SDBS-SWNTs using 660-nm excitation as a function of the  $\text{M}^{2+}$  ionic radius for  $\text{MCl}_2$ ,  $\text{M}(\text{OAc})_2$ , and  $\text{M}(\text{SO}_4)$ .

or electron transfer from the valance band of the SWNT; however, there is clearly a perturbation of the electronic structure of the SWNTs. The intensity of the radial breathing mode (RBM) is an indication of the electron density on the SWNT. In Figure 12, the addition of  $\text{Ba}^{2+}$  shows a reduction in the radial breathing mode (RBM) at  $236\text{ cm}^{-1}$  caused by a loss of electron density in the nanotube.<sup>25,26</sup> The intensity of the RBM undergoes recovery upon the removal of the metal ions. The addition of EDTA (Figure 12c) promotes the formation of a  $\text{M}[\text{EDTA}]$  complex that is sterically hindered from being sufficiently close to the nanotube. On the basis of the foregoing, we propose that the quenching of the fluorescence of SWNTs

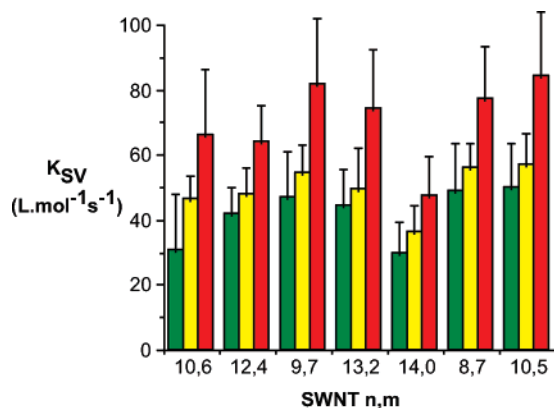


**Figure 9.** Stern–Volmer quenching constants for selected SDBS-SWNT  $n,m$  values (using 660-nm excitation as a function) of the  $X^{n-}$  counterion  $CdX_n$ ,  $X = Cl^-$  (green),  $SO_4^{2-}$  (yellow), and  $OAc^-$  (red).

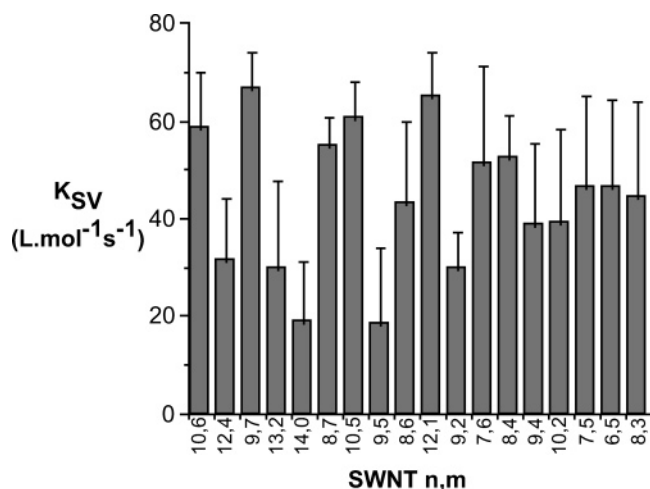


**Figure 10.** Stern–Volmer quenching constants for SDBS-SWNTs (using 660-nm excitation) as a function of SWNT  $n,m$  value in the presence of  $Ca(OAc)_2$ .

is caused, not by a particular electron-transfer process, but rather the distortion of the SWNT's electronic structure by the presence of a charged species in close proximity (contact) to the SWNT.

The optical transitions in SWNTs provide insight into the nature of the excited states in these 1D systems. There has been increasing evidence that light absorption produces strongly correlated electron–hole states in the form of excitons.<sup>1,27,28,29</sup> Bright excitons (those that result in fluorescence) are formed when an electron is excited to a singlet state. Radiative recombination of the electron and hole result in experimentally observed fluorescence. Conversely, if the exciton is a triplet a dark exciton results from which no fluorescence is observed.<sup>30</sup> Swan and co-workers have demonstrated that the local environment around a SWNT shifts the exciton level and also has an effect on the band gap itself.<sup>31</sup> Most of the electric field of the exciton actually flows outside of the SWNT itself and are therefore sensitive to local electric effects. It is also known that the excitons are affected by magnetic fields.<sup>32</sup> The magnetic field shifts the relative levels and can alter the fluorescence intensity; however, the required fields are large. It is clear that the exciton is exquisitely sensitive to its local environment. We propose that even a close approach of such ions should, and indeed does, quench fluorescence. This idea is borne out in recent work by Strano and co-workers,<sup>33</sup> where they use physisorbed ferro/ferricyanide ions to detect peroxide from glucose peroxidase via quenching of fluorescence. In this case, the high charge state quenches fluorescence, yet there is clearly

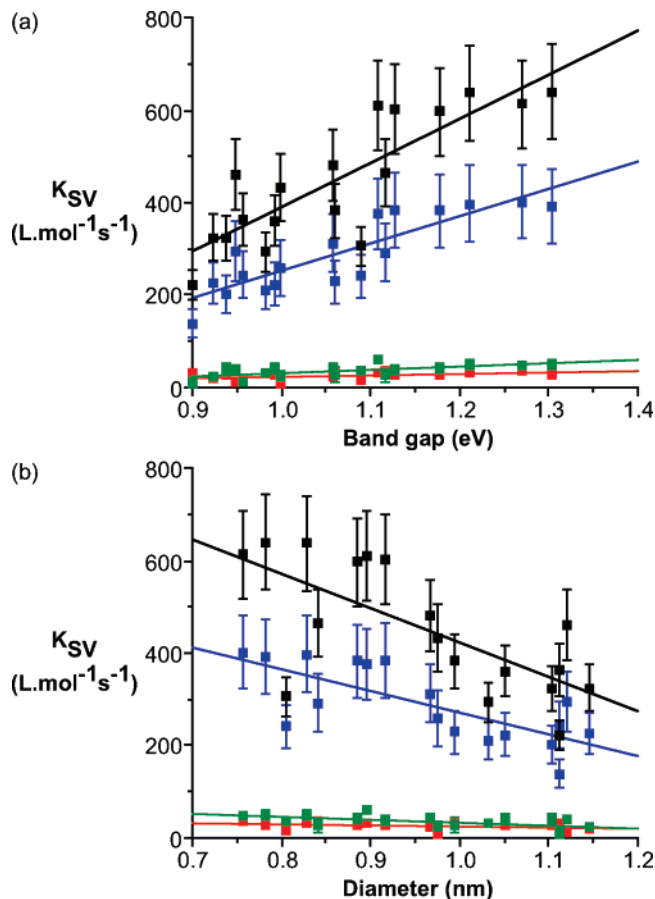


**Figure 11.** Stern–Volmer quenching constants using  $MCl_2$  for selected SDBS-SWNT (using 660-nm excitation) as a function of (a) SWNT band gap and (b) SWNT diameter.  $M = Mg$  (red),  $Ca$  (green),  $Sr$  (blue), and  $Ba$  (black).

not a direct reaction with the SWNT (i.e., covalent bond); the system is reversible and retains the  $[Fe(CN)_6]^{n-}$  structure.

Just as a Coulombic interaction holds an electron–hole pair in close proximity to each other, metal ions present in solution should also interact with excited electrons. If the attractive force is greater for the  $M^{n+} \cdots e^-$  interaction than the  $hole \cdots e^-$  interaction, then the presence of the  $M^{n+}$  ion will cause the radiative recombination of the electron and hole less probable. The excited electron is “pinned” by the charged sphere of the metal ion. This process is observed experimentally as a reduction in fluorescence. It is reasonable to assume that an external perturbation would have a small effect on an electron–hole pair that are spatially close together opposed to an electron and hole that are far apart.

Pedersen has calculated the spatial wave functions of the electron and hole to determine the probability of their location in terms of  $x$  (around the circumference of the SWNT) and  $y$  (along the length of the SWNT).<sup>34</sup> For a small-diameter tube, the probability of finding the electron is distributed pretty evenly around the circumference of the SWNT (i.e., localized in  $y$  but delocalized in  $x$ ). For the large-diameter SWNTs the exciton is localized in both  $x$  and  $y$ , so there is a high probability that the electron and hole are spatially close to each other.

If the quenching involves pinning of the excited electron of the SWNT's electronic structure by a charged species, then this would explain why the sizes of the metal ion and the diameter of the SWNT appear to be the controlling factors. In small-diameter SWNTs, the electron and hole are spatially far from each other. The further the two are apart from each other, then

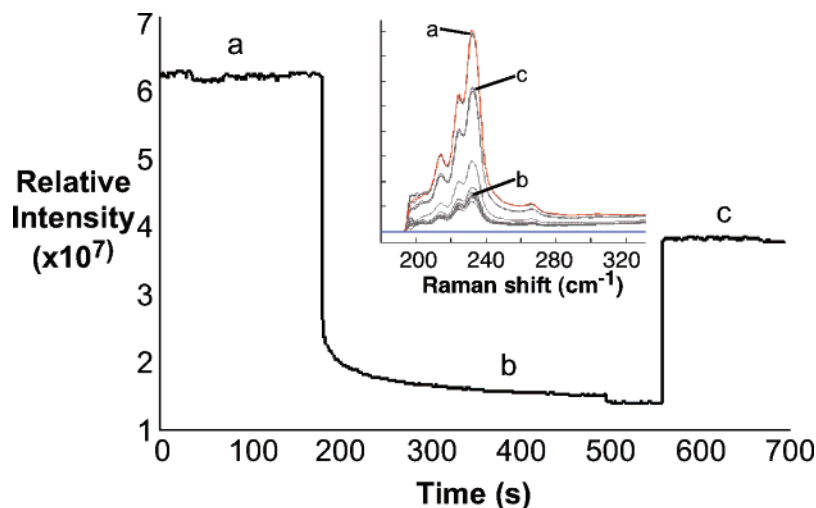


**Figure 12.** Intensity of the radial breathing mode (RBM) as a function of time for (a) SDBS-SWNTs after addition, at  $t = 200$  s, of 0.3 mL 40 mM  $\text{Ba}(\text{OAc})_2$  solution (b), and subsequent addition, at  $t = 550$  s, of 0.3 mL excess EDTA solution (c). The difference in intensity between a and c is consistent with the dilution of the sample.

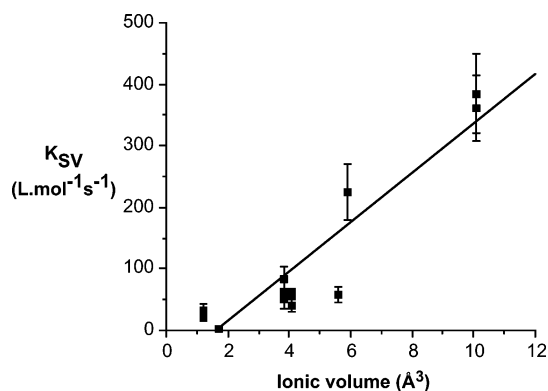


**Figure 13.** Stern–Volmer quenching constant for the 10,5 SDBS-SWNT using 660-nm excitation as a function of the  $\text{M}^{2+}$  ionic volume for  $\text{MCl}_2$ ,  $\text{M}(\text{OAc})_2$ , and  $\text{M}(\text{SO}_4)$  ( $R^2 = 0.859$ ).

the greater chance that an external perturbation can influence the electron and prohibit it from radiative recombination. This would suggest that smaller-diameter nanotubes would be affected greater than larger-diameter SWNTs; this agrees with what we see experimentally. Furthermore, this would also be consistent with the trend that the greatest effect in quenching of fluorescence occurs with the biggest metal ion (i.e.,  $\text{Ba}^{2+}$ ) and the smallest-diameter SWNT (8,3), where the greatest volume of the SWNT's exciton would be affected by the charge of the metal ion. Conversely, the smallest metal ion ( $\text{Mg}^{2+}$ ) would affect only a small fraction of the exciton of the largest-diameter SWNT (12,4). If the quenching of a  $\text{M}^{2+}$  is due to the volume of the charge that subtends the exciton of the SWNT, then for a given SWNT  $n,m$  there should be a correlation between the ionic volume (rather than simply diameter) of the  $\text{M}^{2+}$  ion and the Stern–Volmer quenching constant. Figure 13 shows an example of just such a correlation for the 10,5 SDBS-SWNT.

It should be noted that if charge volume was the only parameter, then the  $\text{Al}^{3+}$  ( $r_{\text{ionic}} = 0.51 \text{ \AA}$ ) and  $\text{Ga}^{3+}$  ( $r_{\text{ionic}} = 0.81 \text{ \AA}$ ) should have quenching efficiencies approaching that for  $\text{Mg}^{2+}$  (0.66  $\text{ \AA}$ ) and  $\text{Cd}^{2+}$  (0.97  $\text{ \AA}$ ), respectively. Given that neither of the group 13 metals shows any appreciable quenching, an alternative reason for their lack of efficacy must be found. At this time, we can propose two possible rationales for the behavior of the group 13 metals. First, if the perturbation of the SWNT's exciton is due to the localization of charge field

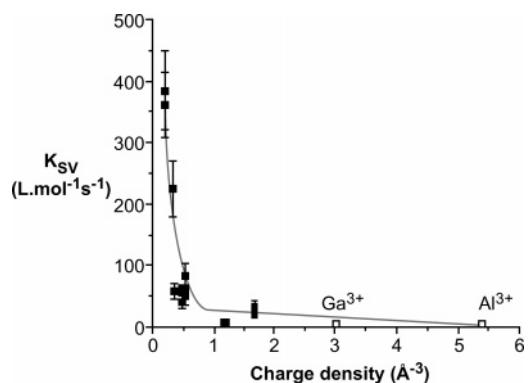


**Figure 14.** Stern–Volmer quenching constant for the 10,5-SDBS-SWNT using 660-nm excitation as a function of the  $\text{M}^{n+}$  charge density for  $\text{M}^{2+}$  (■) and  $\text{M}^{3+}$  (□).

near the SWNT, then both the size of the ion and the magnitude of the charge should be important. In this regard, a plot of Stern–Volmer quenching constant as a function of the  $\text{M}^{n+}$  charge density (Figure 14) shows that the quenching efficiency of  $\text{Al}^{3+}$  and  $\text{Ga}^{3+}$  would be expected to minimal, as indeed is observed. A second explanation may involve the predominant speciation of aluminum and gallium salts in aqueous solution at  $\text{pH} = 10.5$ . Under basic conditions,  $\text{M}(\text{OH})_4^-$  is a significant fraction of the group 13 metal in solution. If the major quenching effect is due to the cationic nature of the metal ions (because the excess  $\text{NH}_3$  dopes the SWNTs with electrons making a  $\text{SWNT} \cdots \text{M}^{n+}$  interaction favored), then the  $\text{M}(\text{OH})_4^-$  would not be expected to quench the fluorescence of the SWNTs. Further studies will be required to elucidate the exact nature of these effects.

## Conclusions

We have demonstrated that diamagnetic group 2 and 12 metal ions quench SDBS-surfacted SWNTs with varying degrees of efficiency. The larger the ionic radii (lower the charge density) of the ion, the greater the efficiencies of quenching; and the smaller the SWNT, the greater the quenching effect of a particular  $\text{M}^{2+}$  ion. The identity of the anion has a lesser effect than that of the metal ion or the diameter (band gap) of the SWNT. We can preclude the formation of a nonfluorescent ground-state complex or spectral bleaching, and propose that

the SWNT excitons formed by light absorption are affected by the presence of the metal ion facilitating nonradiative decay paths.

Our work categorizing metal ions by their charge and radius, and proposing a correlation between the field•••SWNT interactions and quenching rate is consistent with other researcher's views that the SWNT exciton is sensitive to its local environment. We suggest that the highly anisotropic field around the metal ions has a significant effect on the exciton and facilitates nonradiative decay paths. In addition, our data provides a basis for estimating the sensitivity of the fluorescence based on the size and charge density of the various ions employed. We propose that even a close approach of such ions should, and indeed does, quench fluorescence.

Finally, we note that Wang et al.<sup>29</sup> suggested that the excitonic character of optically excited SWNTs "raises the possibility of modifying the SWNT transitions through external perturbations, thus facilitating new electro-optical modulators and sensors." In this regard, we are continuing our studies of the effects of metal ions on the fluorescence of SWNTs and, in particular, the effect of combining electrostatic charge with magnetic field in paramagnetic transition-metal ions.

**Acknowledgment.** The Robert A. Welch Foundation and the National Science Foundation through the Center for Biological and Environmental Nanotechnology provided financial support for this work. We gratefully acknowledge Dr. Howard K. Schmidt (Carbon Nanotube Laboratory, Rice University) for useful discussions. This paper is dedicated to our late colleague Rick Smalley for his leadership in the creation of the first center for nanotechnology in the world, as well as his encouragement in our investigations of SWNTs.

**Supporting Information Available:** Fluorescence spectra with 785-nm excitation and additional plots of Stern–Volmer quenching constants as a function of SWNT band gap and anion. This material is available free of charge via the Internet at <http://pubs.acs.org>.

## References and Notes

- Bachilo, S. M.; Strano, M. S.; Kittrell, C.; Hauge, R. H.; Smalley, R. E.; Weisman, R. B. *Science* **2002**, *298*, 2361.
- Trautman, J. K.; Macklin, J. J.; Brus, L. E.; Betzig, E. *Nature* **1994**, *369*, 40.
- Nirmal, M.; Dabbousi, B. O.; Bawendi, M. G.; Macklin, J. J.; Trautman, J. K.; Harris, T. D.; Brus, L. E. *Nature* **1996**, *383*, 802.
- Kong, J.; Franklin, N. R.; Zhou, C. W.; Chapline, M. G.; Peng, S.; Cho, K. J.; Dai, H. J. *Science* **2000**, *287*, 622.
- Collins, P. G.; Bradley, K.; Ishigami, M.; Zettl, A. *Science* **2000**, *287*, 1801.
- Kong, J.; Chapline, M. G.; Dai, H. J. *Adv. Mater.* **2001**, *13*, 1384.
- O'Connell, M. J.; Eibergen, E. E.; Doorn, S. K. *Nat. Mater.* **2005**, *4*, 412.
- Hariharan, C.; Vijaysree, V.; Mishra, A. K. *J. Lumen.* **1997**, *75*, 205.
- Hariharan, C.; Mishra, A. K. *Radiat. Meas.* **1998**, *29*, 473.
- Grieser, F.; Tausch-Treml, R. *J. Am. Chem. Soc.* **1980**, *102*, 7258.
- Varnes, A. W.; Dodson, R. B.; Wehry, E. L. *J. Am. Chem. Soc.* **1972**, *94*, 946.
- Niyogi, S.; Boukhalfa, S.; Chikkannanavar, S. B.; McDonald, T. J.; Heben, M. J.; Doorn, S. K. *J. Am. Chem. Soc.* **2007**, *129*, 1898.
- Loscutova, R.; Barron, A. R. *J. Mater. Chem.* **2005**, *15*, 4346.
- O'Connell, M. J.; Bachilo, S. M.; Huffman, C. B.; Moore, V. C.; Strano, M. S.; Haroz, E. H.; Rialon, K. L.; Boul, P. J.; Noon, W. H.; Kittrell, C.; Ma, J.; Hauge, R. H.; Weisman, R. B.; Smalley, R. E. *Science* **2002**, *297*, 593.
- It has been observed that  $K_{SV}$  for SWNTs can be dependent on the excitation wavelength, generally weaker at longer excitation wavelength. This has been ascribed to the intrinsic luminescence quantum yield (in the absence of any quencher) decreasing with increasing excitation wavelength, Riggs, J. E.; Guo, Z.; Carroll, D. L.; Sun, Y.-P. *J. Am. Chem. Soc.* **2000**, *122*, 5879.
- Applied NanoFluorescence, Houston, TX.
- We note that the addition of significantly higher concentrations of NaCl has been reported to result in spectral bleaching. See ref 12.
- Tan, Y.; Resasco, D. E. *J. Phys. Chem. B* **2005**, *109*, 14454.
- Strano, M. S.; Huffman, C. B.; Moore, V. C.; O'Connell, M. J.; Haroz, E. H.; Hubbard, J.; Miller, M.; Rialon, K.; Kittrell, C.; Ramesh, S.; Hauge, R. H.; Smalley, R. E. *J. Phys. Chem. B* **2003**, *107*, 6979.
- Dukovic, G.; White, B. E.; Zhou, Z.; Wang, F.; Jockusch, S.; Steigerwald, M. L.; Heinz, T. F.; Friesnew, R. A.; Turro, N. J.; Brus, L. E. *J. Am. Chem. Soc.* **2004**, *126*, 15269.
- Kose, M. E.; Harruff, B. A.; Lin, Y.; Veca, L. M.; Lu, F.; Sun, Y.-P. *J. Phys. Chem. B* **2006**, *110*, 14032.
- Valeur, B. *Molecular Fluorescence: Principles and Applications*; Wiley-VCH, Chichester, 2002.
- Zheng, M.; Diner, B. A. *J. Am. Chem. Soc.* **2004**, *126*, 15490.
- We note that in Figure 2 a slight increase appears in the intensity of the second van Hove transitions with the addition of  $Cd^{2+}$ ; however, this is due to the overlap of the SWNT absorption with the tail of the  $Cd^{2+}$  absorption.
- Kavan, L.; Rapta, P.; Dunsch, L.; Bronikowski, M. J.; Willis, P.; Smalley, R. E. *J. Phys. Chem. B* **2001**, *105*, 10764.
- Okazaki, K.; Nakato, Y.; Murakoshi, K. *Phys. Rev. B* **2003**, *68*, 035434/1.
- Htoon, H.; O'Connell, M. J.; Cox, P. J.; Doorn, S. K.; Klimov, V. I. *Phys. Rev. Lett.* **2004**, *93*, 0027401/1
- Ma, Y.-Z.; Stenger, J.; Zimmermann, J.; Bachilo, S. M.; Smalley, R. E.; Weisman, R. B.; Fleming, G. R. *J. Chem. Phys.* **2004**, *120*, 3368.
- Wang, F.; Dukovic, G.; Brus, L. E.; Heinz, T. F. *Science* **2005**, *308*, 838.
- Dresselhaus, M. S.; Dresselhaus, G.; Saito, R.; Jorio, A. *Annu. Rev. Phys. Chem.* **2007**, *58*, 719.
- Yin, Y.; Cronin, S. B.; Walsh, A.; Stolyarov, A.; Tinkham, M.; Vamivakas, A.; Bacsa, W.; Ünlü, M. S.; Goldberg, B. B.; Swan, A. K. e-print, cond-mat/0505004.
- Zaric, S.; Ostojic, G. N.; Kono, J.; Shaver, J.; Moore, V. C.; Strano, M. S.; Hauge, R. H.; Smalley, R. E.; Wei, X. *Science* **2004**, *304*, 1129.
- Barone, P. W.; Baik, S.; Heller, D. A.; Strano, M. S. *Nat. Mater.* **2005**, *4*, 86.
- Pedersen, T. G. *Phys. Rev. B* **2003**, *67*, 073401–1.